TUDelft

Delft University of Technology

Is Stokes-Einstein relation valid for the description of intra-diffusivity of hydrogen and oxygen in liquid water?
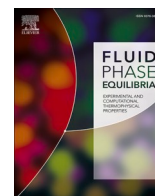
Tsimpanogiannis, Ioannis N.; Moultos, Othonas A.

Important note
To cite this publication, please use the final published version (if applicable).
Please check the document version above.

Is Stokes-Einstein relation valid for the description of intra-diffusivity of hydrogen and oxygen in liquid water?

Ioannis N. Tsimpanogiannis [a],*, Othonas A. Moultos [*],[b]

[a] *Chemical Process & Energy Resources Institute (CPERI), Centre for Research & Technology Hellas (CERTH), Thermi-Thessaloniki, 57001, Greece*
[b] *Engineering Thermodynamics, Process & Energy Department, Faculty of Mechanical, Maritime and Materials Engineering, Delft University of Technology, Leeghwaterstraat 39, 2628CB Delft, the Netherlands*

ARTICLE INFO

ABSTRACT

In this study, all available data from experiments and molecular simulations for the intra-diffusivities of H_2 and O_2 in H_2O, and for the self-diffusivity of pure H_2O are analyzed to examine the validity of the Stokes-Einstein relation. This analysis is motivated by the significant amount of work devoted through the years for improving the predictions of intra- and self-diffusivities in binary and multi-component mixtures relevant to chemical and environmental processes. Here, we calculate the slopes s and t corresponding to the $\ln(D)$ *vs.* $\ln\left(\frac{T}{\eta}\right)$ and $\ln\left(\frac{D}{T}\right)$ *vs.* $\ln\left(\frac{1}{\eta}\right)$ plots, respectively, where D is the intra-diffusivity, η the viscosity, and T the temperature of the systems. Our results show that s and t deviate from unity no matter if the experimental or simulation data are used. This means that the Stokes-Einstein relation is violated for the binary systems of H_2 and O_2 with H_2O, and for pure H_2O. Although prior studies mainly focused on re-evaluating the parameter A of the SE-based semi-theoretical/semi-empirical approaches expressed as $D = A\frac{T}{\eta}$, our results indicate that reliable predictions for the intra- and self-diffusivities can be achieved by improving the accuracy of the prediction of slopes s and t.

1. Introduction

The accurate knowledge of the intra-diffusivity of light gases (e.g., H_2, O_2) in liquid H_2O over a wide range of temperatures and pressures is important for the design and optimization of fuel cells [1] and electrolyzers [2], and for controlling processes such as the air-water gas exchange [3]. The three major routes that are followed for the measurement/estimation of diffusion coefficients are experiments, theoretical/semi-empirical models, and molecular simulations.

At relatively low pressures (e.g., below 1 MPa), the solubilities of H_2 and O_2 in H_2O are rather low [4,5]. For example, the solubility of O_2 in H_2O at atmospheric pressure and temperatures in the range 273.15 – 348.15 K ranges from 3.95×10^{-5} to 1.50×10^{-5} (in mole fractions)[5]. Interestingly, at pressures up to 10 MPa and temperatures up to 333 K, the solubilities can increase by two orders of magnitude. For high pressures (i.e., 100 MPa), the solubilities can increase to a maximum of approximately 1.66×10^{-2}. For a detailed discussion on the effect of pressure on the solubility of O_2 in H_2O the reader is referred to the study by Geng and Duan [6]. In that study, an accurate thermodynamic model to correlate the available experimental measurements has been also presented. A similar behaviour can be observed for the solubilities of H_2 in H_2O [4,7]. Therefore, the intra-diffusivity of these gases in H_2O essentially corresponds to the infinite dilution limit [8].

For conditions at which the solubilities of the gases in H_2O are significantly higher than in the infinite dilution limit, the computation of mutual diffusivities (Fick and Maxwell-Stefan) would be of practical interest since the mass transport occurs due to gradients in chemical potential [9,10]. To this purpose, one can either use Darken equation-based models [9,11,12] or can follow the well-established methodology of computing the Maxwell-Stefan diffusivities (D_{MS}) from the Onsanger coefficients in molecular dynamics (MD) simulations [13–15], and the thermodynamic factor (Γ), e.g., from Kirkwood-Buff integrals [16,17]. Fick diffusivities follow from $D_{Fick} = \Gamma D_{MS}$. In this study, we limit our attention on the diffusivities of infinite diluted gases in H_2O (for which the intra-, Maxwell-Stefan, and Fick diffusivities are all equal [9]).

Usually, very limited experimental diffusivity measurements are available, which are in most cases at/or close to the atmospheric pressure [18]. A detailed discussion on how to overcome this lack of data through the use of semi-empirical approaches is provided elsewhere [10,

---

* Corresponding authors.
  E-mail addresses: i.n.tsimpanogiannis@certh.gr (I.N. Tsimpanogiannis), o.moultos@tudelft.nl (O.A. Moultos).

[12]. Namely, semi-empirical correlations have been extensively used for obtaining the self- and intra-diffusivity values at conditions outside the range of experimental measurements [9–12,19–22]. Such approaches are often guided by the hydrodynamic theory of Stokes-Einstein (SE) [12]. Additional details on SE are provided in Section 2. The accuracy of such semi-empirical methods depends on the extent and quality of the experimental measurements that have been used for their development (i.e., during model calibration). Although, these methods are relatively easy to use and computationally fast, very limited insight into the transport mechanisms occurring in the real system can be extracted. In sharp contrast, approaches such as MD simulations, although being significantly more computationally demanding, can provide detailed physical insight [23,24]. As a result of the ample computational power, the optimized open-source software [25,26], and the accurate intra- and intermolecular potentials available today [27–29], MD has become a reliable and widely used approach for obtaining diffusivities of pure components and mixtures [7,13,30–36], which in turn can be used to devise engineering models and validate the semi-empirical approaches. The purpose of this study is threefold: a) To examine the validity of the SE relation for the intra-diffusivities of H_2 and O_2 in liquid H_2O by utilizing the recent wide collection of MD data [7], b) to perform extensive comparisons with available experimental measurements for the computed values of the SE-associated exponents. While an analysis of the self-diffusion coefficients of pure liquid H_2O has been discussed in detail in recent studies [37–39], this is not the case for the available experimental data regarding the intra-diffusion coefficients of H_2 and O_2 in liquid H_2O. c) To provide guidance to future development/modification of semi-empirical models.

The remainder of this manuscript is organized as follows: In Section 2, the theoretical background is given. In Section 3 the methodology is described. In Section 4, we present the results and discussion for the experimental and MD-based data that are available in the literature. Finally, in Section 5, the conclusions are presented.

2. Theory

The hydrodynamic SE theory directly connects the diffusion coefficient D of a rigid, spherical, Brownian particle in a stationary viscous fluid, to the shear viscosity of the fluid η as follows [40]:

$$D = \frac{kT}{Cr\eta} \tag{1}$$

where k is the Boltzmann constant, T is the temperature of the fluid, and r is the radius of the macroscopic particle. C is a constant that depends on the boundary conditions at the particle/fluid interface. C is equal to 6π when assuming no-slip conditions, e.g., diffusion of very large spherical molecules in solvents of low molecular weight. C is equal to 4π when assuming complete slip conditions, i.e., when the solute and the solvent are identical [21]. In the latter case, D is the self-diffusion coefficient. As pointed out by Poling et al. [12], Eq. (1) strictly applies to macroscopic systems. Eq. (1) holds for simple fluids at relatively high temperatures (i.e., above the melting point of the species) [41]. Although the SE relation is strictly valid only for dilute systems of colloidal particles [42], it has been demonstrated that it works remarkably well for higher densities and for more complex systems. The validity of the SE relation has even been validated for molecular level systems, even though the original theory was derived for a sphere of supermolecular dimensions suspended in a continuous medium (see for example the different systems discussed by Shi et al. [40]). An implied assumption, originating from the initial development [43] of the SE relation, is that the radius of the Brownian particle r is constant (i.e., it does not dependend on T) [44,45]. In this work, we adopt this assumption. It should be noted that in an effort to apply the SE relation to more complex systems, the use of an effective hydrodynamic radius [46] has been proposed [40]. Such an approach, however, could result

in a variable r. This is an issue discussed recently by Ren and Wang [47].

The SE theory has often been used as a guide in developing semi-theoretical models to predict the intra-diffusion coefficients [10,12]. From Eq. (1) we observe that $D \propto \left(\frac{T}{\eta}\right)$. Various semi-theoretical models that have been proposed are often expressed as:

$$D = A\frac{T}{\eta} \tag{2}$$

where A can be a function of various parameters of the system. By taking the logarithm of both sides of Eq. (2)

$$\ln(D) = \ln(A) + \ln\left(\frac{T}{\eta}\right) \tag{3}$$

the "intercept" of the resulting line, (i.e., $\ln(A)$), is associated with the function A, while the "slope" is equal to 1, thus, indicating the validity of the SE relation.

For a detailed discussion on SE-inspired, semi-theoretical models the reader is referred to the extensive review papers of Polling et al. [12], and Kraft and Vogel [48]. Typical examples of such models are the following:

- Wilke-Chang [19], in which

$$A \equiv \frac{7.4 \times 10^{-15}\sqrt{\phi M}}{v_1^{0.6}} \tag{4}$$

where ϕ is the association factor of the solvent (dimensionless), which has a value equal to 2.6 for water, M is the molar mass of the solvent in g/mol.
- Scheibel [49], in which

$$A \equiv \frac{8.2 \times 10^{-15}}{v_1^{1/3}}\left[1 + \left(\frac{3v_2}{v_1}\right)^{2/3}\right] \tag{5}$$

when $v_1 \geq 2.5v_2$, and

$$A \equiv \frac{1.75 \times 10^{-14}}{v_1^{1/3}} \tag{6}$$

when $v_1 < 2.5v_2$.
- Reddy-Doraiswamy [50], in which

$$A \equiv \frac{\Omega\sqrt{M}}{v_1^{1/3}v_2^{1/3}} \tag{7}$$

with $\Omega = 10^{-14}$ when $\frac{v_2}{v_1} \leq 1.5$, while $\Omega = 8.5 \times 10^{-15}$ when $\frac{v_2}{v_1} > 1.5$.
- Lusis-Ratcliff [51], in which

$$A \equiv \frac{8.52 \times 10^{-15}}{v_1^{1/3}}\left[1.4\left(\frac{v_2}{v_1}\right)^{1/3} + \frac{v_2}{v_1}\right]. \tag{8}$$

In Eqs. (4)–(8), v_1 and v_2 are the molar volumes of the solute (component 1) in the solvent (component 2) at their normal boiling

Table 1
Molar mass, normal boiling temperature (at 1 atm), and molar volumes at the normal boiling point for H_2, O_2, and H_2O.

	Molar mass (g/mol)	T_b (K)	V (cm^3/mol)	Reference
H_2	2.016	20.369	14.3	Wilke and Chang [19]
H_2	2.016	20.369	28.45	NIST [52]
O_2	31.199	90.188	25.6	Wilke and Chang [19]
O_2	31.199	90.188	28.04	NIST [52]
H_2O	18.015	373.12	18.9	Wilke and Chang [19]
H_2O	18.015	373.12	18.8	NIST [52]

points at 1 atm. Both molar volumes are in units of cm^3/mol. Table (1) shows the corresponding v_1 and v_2 obtained from NIST [52], as well as the values reported by Wilke and Chang [19] for the three components of interest to this study (i.e., H_2, O_2 and H_2O).

It is evident that these semi-empirical models are based on the assumption that the SE dependency is valid, while a re-evaluation of the function A is performed to improve the performance in predicting the intra-diffusion coefficients. However, this assumption is not always valid. Instead, both model and real fluids have been found to be correlated accurately by the fractional Stokes–Einstein (FSE) relation. This is clearly shown by the extended list of examples discussed by Magalhaes et al. [53] who reviewed the experimental diffusivities of 539 binary systems that contained 8219 data points. According to Harris [54], there are two forms of the FSE encountered in the literature that are of interest to this study:

$$\frac{D}{T} \propto \left(\frac{1}{\eta}\right)^t \tag{9}$$

$$D \propto \left(\frac{T}{\eta}\right)^s \tag{10}$$

where the exponents t and s can be determined from the slope of the corresponding log–log plot. When t or s are equal to 1, the SE relation is valid. When $t \neq 1$ (or $s \neq 1$), SE relation is violated and, thus, the FSE is valid. The non-universal fractional exponents are an indication of the decoupling between D and η. In that case, D and η are determined by different time scales. This decoupling is associated with the development of mesoscopic structured regions which have slower dynamics with respect to the system average. On the other hand, when the SE relation is valid (i.e., the exponents are equal to one) they are determined by the same time scale [41,55], and therefore, D and η are coupled (especially at higher temperatures). The inherent assumption behind both of the aforementioned variants of the SE relation is that the radius of the diffusing particle r is constant [56]. Zhao and Zhao [56] reported examples of systems that violate the SE relation, such as supercooled or glass-forming liquids, dense complex media, and low-density gases. In the same study [56], the size and mass dependence of the SE relation was computationally investigated by decomposing the kinetic and hydrodynamic contributions to D. Additional discussion and related references can be also found in our earlier studies [38,39].

A characteristic example of the validity of FSE is the self-diffusivity of pure water. Harris [54] reported the following absolute values for the exponent t, based on available experimental measurements: 0.9429 for $623 \geq T \geq 274$, and 0.6684 for $273 \geq T \geq 238$ (where T is in units of K).

Tsimpanogiannis et al. [39] pointed out the importance of self-consistency in the experimental measurements or data computed in MD simulations when examining the validity (or violation) of the SE relation. In particular, diffusivity (intra- or self-) and shear viscosity should be both either measured experimentally, or both be computed in MD simulations using the same force fields. When MD simulations are performed, systems having more than 1000 molecules should be used, or a Yeh-Hummer [57,58] type correction should be implemented in order to account for system size effects (SSE). As discussed in detail in a number of studies (e.g., Dünweg and Kremer [59], Yeh and Hummer [57], Jamali et al. [15,60], Celebi et al. [58], Erdős et al. [61]) the magnitude of the required correction to mitigate the SSE strongly depends on the type of system and the thermodynamic conditions. The computation of η using MD simulations does not depend on the system size [57,62,63].

3. Methodology - data selection

In the current study no new experimental measurement or MD simulation is performed. Instead, recent literature-reported data are utilized for the analysis. The extensive experimental data reviewed by

Tsimpanogiannis et al. [7] are used in the this study to examine the validity of the SE relation for the diffusivity of H_2 or O_2 in H_2O. Since the experimentally measured self-diffusivities of H_2O have been discussed in detail in a number of studies [54,64], no further discussion is presented here. The analysis for the MD simulations is based primarily on the recent, new simulations reported by Tsimpanogiannis et al. [7], which span a wide temperature (275.15–975.15 K) and pressure (0.1–200 MPa) range.

For both experimental and MD data, the two forms of the FSE are examined (i.e., Eqs. (9)–(10)). The exponents t or s are determined from the slope of the corresponding log–log plot. Namely,

- $\ln\left(\frac{D}{T}\right)$ *vs.* $\ln\left(\frac{1}{\eta}\right)$, and
- $\ln(D)$ *vs.* $\ln\left(\frac{T}{\eta}\right)$

are used for the calculation of the exponents t or s, respectively. Tables 3 and 4 list all calculated values (experimental/MD) for the case of the intra-diffusivities of H_2 and O_2 in H_2O, respectively, while Table 5 lists the corresponding values for the case of the self-diffusivities of pure H_2O.

3.1. MD simulations

To compute the intra-diffusivities of H_2 and O_2 in H_2O, Tsimpanogiannis et al. [7] examined the combination of six H_2 and six O_2 force fields with the TIP4P/2005 H_2O force field [27]. These combinations were evaluated based on the performance in predicting the density, self-diffusion coefficients and viscosities of the pure gases, and the self-diffusion coefficients of the gases in H_2O at low pressures. It was concluded that the Buch [65] - TIP4P/2005 and the Bohn et al. [66] - TIP4P/2005 force field combinations were the most accurate. Subsequently, these force fields were used to compute the intra-diffusion coefficients of H_2 and O_2 in H_2O for a wide temperature and pressure range spanning vapor, liquid and supercritical conditions. In this study, the MD data [7] corresponding to H_2 and O_2 diffusion in liquid H_2O are further analyzed.

3.2. Experimental data

3.2.1. H_2 in H_2O

Himmelblau [18] and Winkelmann [67] presented detailed reviews on the available experimental data for the H_2 intra-diffusion coefficients in H_2O as a function of temperature at 0.1 MPa. Moreover, Tsimpanogiannis et al. [7] analysed the experimental data reported by Gertz and Loeschcke [68], Baird and Davidson [69], Wise and Houghton [70], Akgerman and Gainer [71], de Blok and Fortuin [72], Verhallen et al. [73] and Jähne et al. [3] and identified that the majority fell onto two distinct Arrhenius-type curves (denoted in the current study as "high curve" and "low curve"), with some experimental data falling in-between the two curves. The two curves differed by approximately 70%. The Arrhenius-type curves were described using an equation [9, 12] of the type:

$$D = Do \exp\left(\frac{\alpha}{T}\right) \tag{11}$$

where D_o and α were fitting parameters. The reported values of the parameters for the two curves are listed in Table 2. It is common to

Table 2
Parameters of the Arrhenius fit (Eq. (11)) to the experimental data of H_2 in H_2O at 1 atm.

	$\ln(D_o)$	α
"High Curve"	-12.22 ± 0.48	$(-0.199 \pm 0.014) \times 10^4$
"Low Curve"	-13.29 ± 0.37	$(-0.181 \pm 0.011) \times 10^4$

Table 3
Collective results for the slopes and intercepts of the SE theory calculated for the case of the intra-diffusion of H_2 in H_2O. The numbers in the parentheses are the standard deviations.

	$\ln(D)$ as function of $\ln(T/\eta)$		$\ln(D/T)$ as function of $\ln(1/\eta)$	
	slope (s)	intercept (s)	slope (t)	intercept (t)
Experimental (this work, all temperatures)	0.784 (0.045)	-29.338 (0.576)	0.753 (0.511)	-30.345 (0.366)
Experimental (this work, 273.15 – 298.65 K)	0.787 (0.097)	-29.371 (1.221)	0.761 (0.110)	-30.400 (0.756)
Experimental (this work, 302.15 – 333.15 K)	0.766 (0.081)	-29.099 (1.048)	0.725 (0.094)	-30.145 (0.688)
Expt. fit ("high curve", all temperatures)	0.920 (0.007)	-30.581 (0.095)	0.905 (0.008)	-30.935 (0.061)
Expt. fit ("high curve", 274 – 298 K)	0.781 (0.007)	-28.842 (0.081)	0.753 (0.007)	-29.896 (0.047)
Expt. fit ("high curve", 300 – 372 K)	0.984 (0.005)	-31.451 (0.064)	0.980 (0.006)	-31.518 (0.043)
Expt. fit ("low curve", all temperatures)	0.838 (0.007)	-30.006 (0.087)	0.809 (0.007)	-30.728 (0.054)
Expt. fit ("low curve", 274 – 298 K)	0.711 (0.006)	-28.421 (0.074)	0.675 (0.006)	-29.811 (0.042)
Expt. fit ("low curve", 300 – 372 K)	0.896 (0.004)	-30.798 (0.058)	0.875 (0.005)	-31.242 (0.038)
MD (this work, 275.15 – 637.15 K)	0.869 (0.014)	-30.339 (0.199)	0.828 (0.017)	-30.786 (0.142)
MD (this work, 298.15 – 637.15 K)	0.915 (0.014)	-31.012 (0.195)	0.886 (0.018)	-31.288 (0.148)

express α as $\frac{-E_a}{R}$, where E_a is the activation energy for diffusion and R is the universal gas constant. Tsimpanogiannis et al. [7] recommended the adoption of the experimental data falling on the "low curve" curve since they exhibited the least deviation from the MD results using the most accurate force field combination for the system H_2 - H_2O (i.e., Buch [65] - TIP4P/2005 [27]).

3.2.2. O_2 in H_2O

Similarly, for the case of O_2 diffusing in H_2O, Himmelblau [18] presented an earlier review, while Tsimpanogiannis et al. [7] used the following additional experimental data, reported by Gertz and Loeschcke [68], Baird and Davidson [69], Wise and Houghton [70], Ferrell and Himmelblau [74], Akgerman and Gainer [71], and Han and Bartels [75]. A similar pattern to the H_2 - H_2O system was identified by Tsimpanogiannis et al. [7]. Namely, that the majority of the experimental data fell onto two distinct curves ("high curve" and "low curve"). Essentially, the "low curve" consisted primarily only of the data from the experimental study by Han and Bartels [75]. The two curves differed by

approximately 25%. Tsimpanogiannis et al. [7] recommended the adoption of the experimental data falling on the "high curve" since they exhibited the least deviation from the MD results using the most accurate force field combination for the system O_2 - H_2O (i.e., Bohn [66] - TIP4P/2005 [27]).

4. Results and discussion

4.1. MD simulations

Figure 1 shows the validity test of the Stokes–Einstein relation, $D \propto \left(\frac{T}{\eta}\right)$, for the intra-diffusivities of H_2 in H_2O (Fig. 1a), O_2 in H_2O (Fig. 1b), and the self-diffusivities of pure H_2O (Fig. 1c) based on the MD data reported by Tsimpanogiannis et al. [7]. The data used in Fig. 1 include all the MD simulations in the temperature range 275.15–637.15 K and pressure range 0.1–200 MPa, and correspond to conditions where the solvent (i.e., H_2O) is in the liquid state. Although the experimentally measured critical temperature T_c and pressure P_c of H_2O are 647.096 K

Table 4
Collective results for the slopes and intercepts of the SE theory calculated for the case of the intra-diffusion of O_2 in H_2O. The numbers in the parentheses are the standard deviations.

	$\ln(D)$ as function of $\ln(T/\eta)$		$\ln(D/T)$ as function of $\ln(1/\eta)$	
	slope (s)	intercept (s)	slope (t)	intercept (t)
Experimental (this work, all temperatures)	0.982 (0.045)	-32.308 (0.575)	0.978 (0.052)	-32.389 (0.370)
Experimental (this work, 283.15 – 298.65 K)	0.914 (0.171)	-31.454 (2.140)	0.903 (0.194)	-31.868 (1.329)
Experimental (this work, 302.15 – 333.15 K)	1.029 (0.083)	-32.923 (1.082)	1.033 (0.097)	-32.792 (0.713)
Exp. Fit ("high curve", all temperatures)	0.899 (0.003)	-31.206 (0.044)	0.882 (0.004)	-31.662 (0.031)
Exp. Fit ("high curve", 275 – 299 K)	0.926 (0.002)	-31.546 (0.024)	0.916 (0.002)	-31.903 (0.014)
Exp. Fit ("high curve", 301 – 373 K)	0.871 (0.004)	-30.826 (0.058)	0.846 (0.006)	-31.382 (0.042)
MD (this work, 275.15 – 637.15 K)	0.917 (0.010)	-31.603 (0.147)	0.893 (0.013)	-31.902 (0.111)
MD (this work, 298.15 – 637.15 K)	0.911 (0.115)	-31.511 (0.166)	0.884 (0.015)	-31.821 (0.127)

Table 5
Collective results for the slopes and intercepts of the SE theory calculated for the case of the self-diffusion of pure H_2O. The numbers in the parentheses are the standard deviations.

|	$\ln(D)$ as function of $\ln(T/\eta)$		$\ln(D/T)$ as function of $\ln(1/\eta)$	
	slope (s)	intercept (s)	slope (t)	intercept (t)
Experimental (Dehaoui et al. [64], 274 – 373 K)	0.95	-31.968	0.941	-32.192
Experimental (Harris [54], 274 – 623 K)	-	-	0.943	-4.977
MD (Moultos et al. [8], 298 – 623 K)	0.977	-32.493	0.968	-32.509
MD (Tsimpanogiannis et al. [38], 280 – 623 K)	0.934	-31.793	0.913	-32.017
MD (this work, 275.15 – 637.15 K)	0.920 (0.076)	-31.549 (0.108)	0.895 (0.009)	-31.823 (0.077)
MD (this work, 298.15 – 637.15 K)	0.947 (0.007)	-31.940 (0.095)	0.929 (0.009)	-32.115 (0.073)
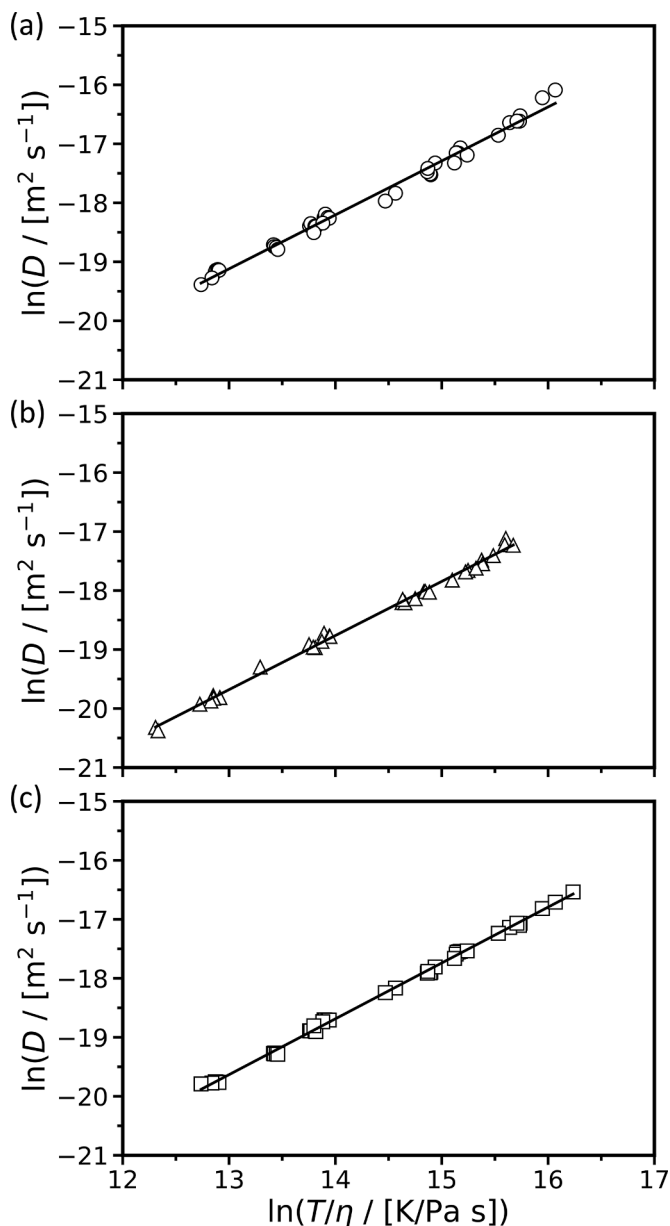
Fig. 1. Validity test of the SE theory for the MD simulations reported by Tsimpanogiannis et al. [7] for the cases of: a) H_2 intra-diffusion coefficient in H_2O, b) O_2 intra-diffusion coefficient in H_2O, and c) pure H_2O self-diffusion coefficient. The Buch [65], Bohn [66] and TIP4P/2005 [27] force fields were used for the H_2, O_2 and H_2O, respectively. Symbols denote the MD simulations, while the solid lines denote the linear fit used for the calculation of the slope s. The error bars are comparable or smaller than the symbol size. The statistical uncertainties of the computed diffusivities can be found in Ref. [7].

and 22.064 MPa [76], respectively, in order for our analysis to be self-consistent, it is based on the critical point of the TIP4P/2005 H_2O force field which corresponds to a temperature of 640 K and a pressure of 14.6 MPa [77]. The values for the slopes, s and t, corresponding to the MD simulations for all systems in this study, are reported in Tables 3 (H_2 in H_2O), 4 (O_2 in H_2O) and 5 (pure H_2O). The exponent s can be extracted from the slopes of the fitted lines for the three cases shown in Fig. 1. The coefficients of determination, R^2, for the fits are equal to 0.991, 0.996, and 0.998 for the cases of H_2 in H_2O, O_2 in H_2O, and pure H_2O, respectively. These values indicate an excellent fit. We observe that for the case of the intra-diffusivity of H_2 in H_2O the calculated slope is $s = 0.915 \pm 0.014$, while for the case of O_2 in H_2O the slope is $s =$

0.911 ± 0.115 The corresponding values for the slope t can be calculated from $\ln\left(\frac{D}{T}\right)$ *vs* $\ln\left(\frac{1}{\eta}\right)$ plots, and the resulting values can be found in Tables 3 and 4. The calculated values of s and t remain practically insensitive for all the fitted temperature ranges considered. Tables 3, 4 and 5 show the results for two different temperature ranges; namely, 275.15–637.15 K and 298.15–637.15 K. Other temperature ranges that have been considered, resulted in similar values for the slopes (i.e., having an absolute deviation of less than 4% for both cases of O_2 or H_2 diffusing in H_2O).

As far as the self-diffusivity of pure H_2O is concerned, the calculated slopes (i.e., $s = 0.947 \pm 0.007$ and $t = 0.929 \pm 0.009$) are in very good agreement with the values reported previously in the studies by Moultos et al. [8] and Tsimpanogiannis et al. [39] (see Table 5). For the slope s, we observe an absolute deviation equal to 1.34% between this study and Tsimpanogiannis et al. [39], and 3.17% between this study and Moultos et al. [8]. The respective values for the slope t are 1.73% and 4.19%. As also shown in Table 5, an excellent agreement is observed between the slope values resulting from the MD simulations and those reported for the experimental measurements by Dehaoui et al. [64] and Harris [54] (i.e., absolute deviation equal to less than 1.5%).

Our analysis clearly indicates that the reported MD simulations for the three systems considered [i.e., the intra-diffusion of H_2 (Buch [65]) or O_2 (Bohn et al. [66]) in liquid H_2O (TIP4P/2005 [27]), and the self-diffusion of pure H_2O (TIP4P/2005 [27])] violate the SE equation. Additional discussion and comparisons are provided in the following Sections.

4.2. Experimental data

Figure 2 shows the validity test of the Stokes–Einstein relation, given by Eq. (10), $D \propto \left(\frac{T}{\eta}\right)$, for the available experimentally measured intra-diffusivities of H_2 in H_2O at a pressure of 1 atm and temperatures in the range 273.15–333.15 K. For all the experimental data-sets shown in Fig. 2, the respective values of the slopes and intercepts are listed in Table 6. The values of slope s vary in the range 0.719–1.289. Fig. 3 shows the validity test of the Stokes–Einstein relation for all available experimental data of the intra-diffusivities of O_2 in H_2O at a pressure of 1 atm and temperatures in the range 283.15–333.15 K. The corresponding calculated values for the slopes and intercepts are listed in Table 7. For this system, the values for the slope s vary from 0.803 to 1.334.
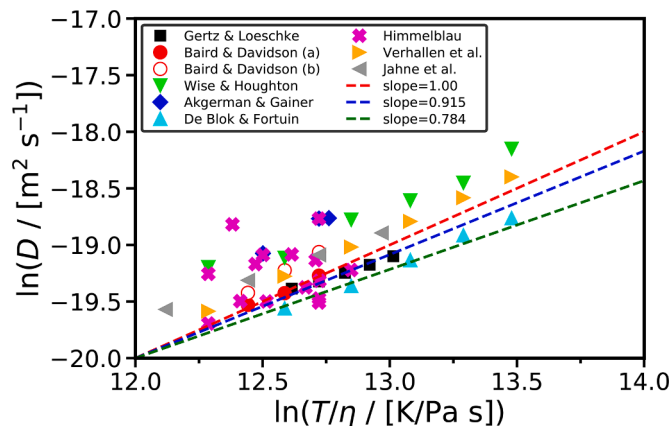

Fig. 2. Validity test of the SE theory for the experimental data of H_2 intra-diffusion coefficient in H_2O. Sources of experimental data: Gertz and Loeschcke [68], Baird and Davidson [69], Wise and Houghton [70], Akgerman and Gainer [71], de Blok and Fortuin [72], Winkelmann [67], Himmelblau [18], Verhallen et al. [73] and Jähne et al. [3]. The dashed lines indicate the different slopes of interest: $s = 1.000$ – red; $s = 0.915$ – blue; $s = 0.784$ – green. (For interpretation of the references to colour in this figure legend, the reader is referred to the web version of this article.)

Table 6

Calculated slopes s and t for the case of the experimental intra-diffusion of H_2 in H_2O. The numbers in the parentheses are the standard deviations.

|	ln(D) as function of ln(T/η)		ln(D/T) as function of ln($1/\eta$)	
	slope (s)	intercept (s)	slope (t)	intercept (t)
Gertz and Loeschcke [68]	0.719 (0.023)	-28.459 (0.289)	0.676 (0.025)	-29.758 (0.181)
Baird and Davidson (a) [69]	0.920 (0.123)	-30.985 (1.543)	0.909 (0.140)	-31.361 (0.963)
Baird and Davidson (b)[69]	1.289 (0.055)	-35.462 (1.289)	1.330 (0.062)	-34.097 (0.429)
Wise and Houghton [70]	0.881 (0.082)	-30.101 (1.056)	0.861 (0.094)	-30.640 (0.678)
Akgerman and Gainer [71]	1.267 (0.162)	-34.910 (2.055)	1.305 (0.185)	-33.656 (1.290)
de Blok and Fortuin [72]	0.916 (0.030)	-31.104 (0.392)	0.901 (0.035)	-31.483 (0.255)
Verhallen et al. [73]	0.993 (0.005)	-31.782 (0.060)	0.992 (0.005)	-31.814 (0.039)
Jähne et al. [3]	0.796 (0.002)	-29.218 (0.019)	0.768 (0.002)	-30.184 (0.015)
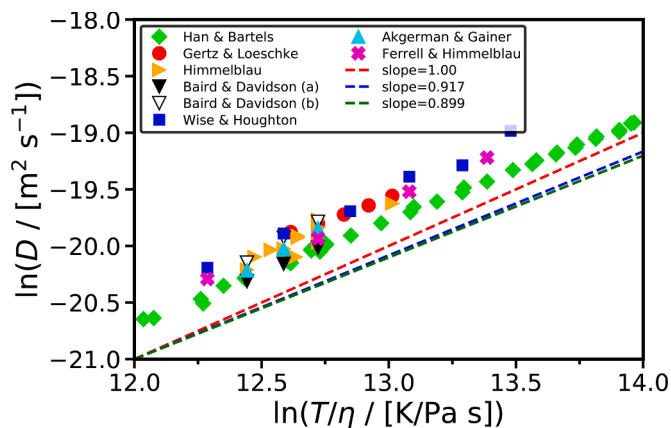
Fig. 3. Validity test of the SE relation for the experimental data of O_2 intra-diffusion coefficient in H_2O. Sources of experimental data: Han and Bartels [75], Gertz and Loeschcke [68], Baird and Davidson [69], Wise and Houghton [70], Akgerman and Gainer [71], Ferrell and Himmelblau [74] and Himmelblau [18]. The dashed lines indicate the different slopes of interest: $s = 1.000$ – red; $s = 0.917$ – blue; $s = 0.899$ – green. (For interpretation of the references to colour in this figure legend, the reader is referred to the web version of this article.)

Table 7

Calculated slopes s and t for the case of the experimental intra-diffusion of O_2 in H_2O. The numbers in the parentheses are the standard deviations.

|	ln(D) as function of ln(T/η)		ln(D/T) as function of ln($1/\eta$)	
	slope (s)	intercept (s)	slope (t)	intercept (t)
Gertz and Loeschcke [68]	0.803 (0.024)	-30.018 (0.303)	0.773 (0.027)	-30.926 (0.191)
Wise and Houghton [70]	0.980 (0.052)	-32.242 (0.674)	0.976 (0.060)	-32.311 (0.434)
Ferrell and Himmelblau [74]	0.989 (0.049)	-32.469 (0.627)	0.987 (0.056)	-32.516 (0.402)
Baird and Davidson (a) [69]	1.059 (0.001)	-33.490 (0.011)	1.067 (0.001)	-33.211 (0.006)
Baird and Davidson (b) [69]	1.290 (0.145)	-36.180 (1.822)	1.330 (0.164)	-34.815 (1.134)
Akgerman and Gainer [71]	1.334 (0.006)	-36.818 (0.074)	1.381 (0.007)	-35.240 (0.051)
Han and Bartels [75]	0.910 (0.006)	-31.611 (0.076)	0.895 (0.007)	-32.017 (0.051)
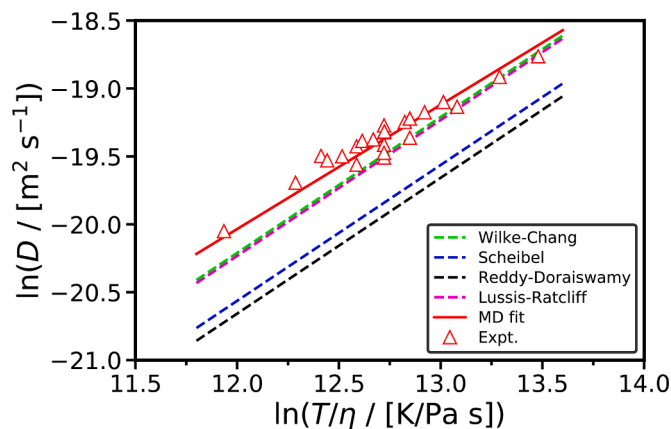
Fig. 4. Comparison of the experimental data (denoted with red triangles) of H_2 intra-diffusion coefficient in H_2O, recommended by Tsimpanogiannis et al. [7]. The red solid line indicates the fitted line with slope equal to $s = 0.784 \pm 0.045$. The dashed lines indicate the calculations with four semi-theoretical models (Wilke and Chang [19] - dashed blue line; Scheibel [49] - dashed green line; Reddy and Doraiswamy [50] - dashed magenta line; and Lussis and Ratcliff [51] - dashed black line). The error bars are comparable or smaller than the symbol size. The statistical uncertainties of the computed diffusivities can be found in Ref.[7]. (For interpretation of the references to colour in this figure legend, the reader is referred to the web version of this article.)
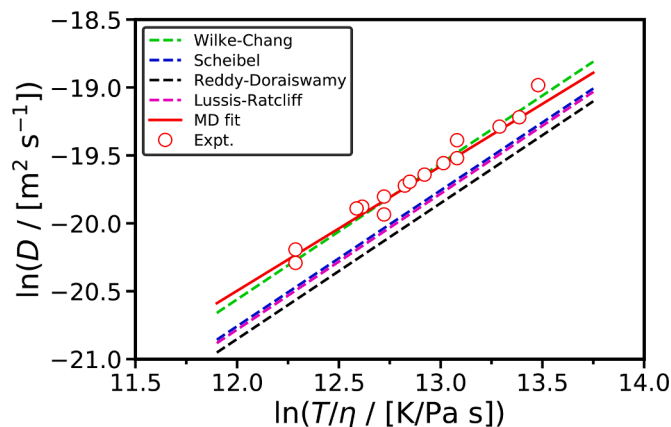

Fig. 5. Comparison of the experimental data (denoted with red triangles) of O_2 intra-diffusion coefficient in H_2O, recommended by Tsimpanogiannis et al. [7]. The red solid line indicates the fitted line with slope equal to $s = 0.982 \pm 0.045$. The dashed lines indicate the calculations with four semi-theoretical models (Wilke and Chang [19] - dashed blue line; Scheibel [49] - dashed green line; Reddy and Doraiswamy [50] - dashed magenta line; and Lussis and Ratcliff [51] - dashed black line). (For interpretation of the references to colour in this figure legend, the reader is referred to the web version of this article.)

Fig. 4 shows the corresponding validity test of the SE relation for the case of the intra-diffusivities of H_2 in H_2O using only the experimental data-sets that follow closely the "low curve" discussed in Section 4.1. The red solid line indicates a fit to the selected experimental data with an overall slope of $s = 0.784 \pm 0.045$. Similarly, Fig. 5 shows the corresponding validity test of the SE relation for the case of the intra-diffusivities of O_2 in H_2O using only the experimental data-sets that follow closely the "high curve" discussed in Section 4.1. The red solid line is a fit to the selected experimental data within an overall slope of $s = 0.982 \pm 0.045$.

From our analysis it is observed that there is some disagreement between the values for the slopes, s, that are calculated from the MD data and those using the experimental data for the cases of the intra-diffusivities of H_2 or O_2 in H_2O (see also Tables 3 and 4). The absolute

deviation for *s*, for the diffusivity of H_2 in H_2O is 9.78%, while for O_2 in H_2O is 7.09%. The corresponding absolute deviations for the slopes, *t*, are 9.06% and 9.52%, respectively. To further investigate the origins of this disagreement, the slopes *t* and *s* are recalculated using values for the intra-diffusivites from the reported correlations (i.e., ln*D vs. T*), instead of using all the experimental data. As can be seen in Tsimpanogiannis et al. [7], the experimental data are not evenly distributed for the various temperatures, with a higher number of scattered data being around or lower than the temperature of 298 K (see also Figs. 2 and 3). After the re-evaluation we observe that for the case of O_2 intra-diffusion in H_2O, the absolute deviation of the slope *s* between the MD simulations and the experimental data fit drops to 1.96%. An improved, yet more complex behavior, is observed for H_2 intra-diffusion in H_2O; The reported MD data follow more closely the "high curve" for temperatures up to 298 K, while they follow more closely the "low curve" for all temperatures that are higher than 298 K. This was the main reason that ref [7] recommended the adoption of the data following the "low curve".

To further investigate the source of the observed disagreement between the slopes *s* obtained using the MD data and the experiments, the slopes *t* and *s* are recalculated using values for the intra-diffusivites from the reported correlations using two different temperature ranges; namely, 274–298 K and 300–372 K. We observe that the calculated slope from the "low curve" in the temperature range 300–372 K is equal to $s = 0.896 \pm 0.004$ which is in a very good agreement (absolute deviation equal to 2.08%) with the MD-based value (i.e., $s = 0.915 \pm 0.014$) that was calculated here using the MD data reported by Tsimpanogiannis et al. [7].

4.3. Comparison with other literature values

Two types of comparisons are considered here. First, we compare the four semi-empirical models (i.e., Wilke and Chang [19], Scheibel [49], Reddy and Doraiswamy [50], and Lusis and Ratcliff [51]) with the selected experimental data. Figure 4 shows the comparison for H_2 intra-diffusion in H_2O, while Fig. 5 shows the comparison for O_2 intra-diffusion in H_2O. From Fig. 4 we observe that the Wilke and Chang model gives essentially identical predictions with the Lusis and Ratcliff model. The predictions of both models are in very good agreement with the experimental data at higher temperatures, while the agreement decreases at lower temperatures as a result of the semi-empirical models having a different slope *s* from the experimental data. The predictions from the Scheibel and the Reddy and Doraiswamy models have a higher deviation, with the latter model being the least accurate. From Fig. 5 we observe that the Wilke and Chang model goes through the experimental data for the entire temperature range, having a slope *s* equal to 1 (obeying the SE relation), while the experimental data have a slope equal to 0.899 ± 0.003. The predictions of the other three models are almost identical, deviating from the experimental data.

Second, we compare the calculated *s* and *t* with other reported values from the literature. Magalhães et al. [53] reported an extensive collection of intra-diffusion coefficients for various binary systems, including the two binary systems discussed here. The authors correlated the experimental data with nine different relations, including the two forms of the FSE (i.e., Eqs. (9) and (10)) that are considered here. For the intra-diffusivity of H_2 in H_2O, Magalhães et al. [53] used only the experimental data of Jähne et al. [3] and reported the values of 0.81581 ± 0.02468 and 0.78958 ± 0.02669 for the slopes *s* and *t*, respectively. These values are in very good agreement with the ones listed in Table 6. For intra-diffusivity of O_2 in H_2O, Magalhães et al. [53] used the data of Han and Bartels [75] (i.e., 36 experimental data points) and Wise and Houghton (i.e., 4 experimental data points) and reported the values of 0.90980 ± 0.01337 and 0.89400 ± 0.01591 for the slopes *s* and *t*, respectively. These are essentially identical with the values for Han and Bartels [75] experimental data that are shown in Table 7. This outcome is expected since the experimental data from Han and Bartels consist 90% of all the experimental data used for the slope calculations

by Magalhães et al. [53]. It is also interesting to observe that the calculated slopes from the experimental data from Han and Bartels are in excellent agreement with the slopes from the MD simulations. However, the Han and Bartels values for the diffusion coefficient are shifted to lower values by 25%.

5. Conclusions

Significant effort has been devoted in the literature for creating models that can accurately predict the experimentally measured intra-diffusion coefficients of numerous binary mixtures encountered in industrial applications. The primary focus of earlier studies has been on the re-evaluation of the parameter *A* that is encountered in SE-based semi-theoretical/semi-empirical approaches expressed as $D = A \cdot \frac{T}{\eta}$. By plotting $\ln(D)$ as a function of $\ln\left(\frac{T}{\eta}\right)$, or $\ln\left(\frac{D}{T}\right)$ as a function of $\ln\left(\frac{1}{\eta}\right)$ the respective slopes *s* and *t* can be calculated. Slope values equal to one indicate the validity of the SE relation. As clearly shown in this study for the intra-diffusivities of H_2 and O_2 in H_2O, and for the self-diffusivity of pure H_2O, to enhance the accuracy of the prediction of intra-diffusivities it is essential to shift the focus from parameter *A* to describing the slope *s* (or *t*) more accurately. Here, we use all the available data from experiments and MD simulations. Our analysis clearly indicates that the SE relation is violated for both the MD simulation data and the experimental measurements. A good agreement is found for the newly-calculated slopes *s* and *t*, between the MD simulations and the experimental data. Here, we focused on the analysis of intra-diffusivities of infinite diluted gases in H_2O. A thorough investigation of the validity of SE in systems where collective diffusivities (Maxwell-Stefan and Fick) are relevant (e.g., for high gas compositions, multi-component mixtures, electrolyte solutions) can be a natural extension of this work [78–82]. Finally, a study of the implications of our findings for fluids confined into nano- and meso-porous materials [83–86], where models such as the Maxwell-Stefan have been applied, would be an interesting future outlook.

Data Availability

Is Stokes-Einstein relation valid for the description of intra-diffusivity of hydrogen and oxygen in liquid water? (Mendeley Data)

CRediT authorship contribution statement

Ioannis N. Tsimpanogiannis: Conceptualization, Data curation, Methodology, Visualization, Writing – original draft, Writing – review & editing. **Othonas A. Moultos:** Conceptualization, Data curation, Methodology, Visualization, Writing – original draft, Writing – review & editing.

Declaration of Competing Interest

None.

References

[1] M. Ball, M. Wietschel, The future of hydrogen - opportunities and challenges, Int. J. Hydrog. Energy 34 (2) (2009) 615–627.

[2] A. Ursua, L.M. Gandia, P. Sanchis, Hydrogen production from water electrolysis: current status and future trends, Proc. IEEE 100 (2) (2012) 410–426.

[3] B. Jähne, G. Heinz, W. Dietrich, Measurement of the diffusion coefficients of sparingly soluble gases in water, J. Geophys. Res. Oceans 92 (C10) (1987) 10767–10776.

[4] R. Battino, IUPAC Solubility Data Series. Vol 7. Hydrogen and Deuterium, first ed., Pergamon Press, Oxford, 1981.

[5] C.L. Young, IUPAC Solubility Data Series. Vol 5/6. Oxygen and Ozone, first ed., Pergamon Press, Oxford, 1981.

[6] M. Geng, Z. Duan, Prediction of oxygen solubility in pure water and brines up to high temperatures and pressures, Geochim. Cosmochim. Acta 74 (19) (2010) 5631–5640.

[7] I.N. Tsimpanogiannis, S. Maity, A.T. Celebi, O.A. Moultos, Engineering model for predicting the intradiffusion coefficients of hydrogen and oxygen in vapor, liquid, and supercritical water based on molecular dynamics simulations, J. Chem. Eng. Data 66 (8) (2021) 3226–3244.

[8] O.A. Moultos, I.N. Tsimpanogiannis, A.Z. Panagiotopoulos, I.G. Economou, Atomistic molecular dynamics simulations of CO₂ diffusivity in H₂O for a wide range of temperatures and pressures, J. Phys. Chem. B 118 (20) (2014) 5532–5541.

[9] R. Taylor, R. Krishna, Multicomponent Mass Transfer, first ed., John Wiley & Sons, New York, 1993.

[10] E.L. Cussler, Diffusion: Mass Transfer in Fluid Systems, third ed., Cambridge University Press, Cambridge, 2009.

[11] L. Wolff, S.H. Jamali, T.M. Becker, O.A. Moultos, T.J.H. Vlugt, A. Bardow, Prediction of composition-dependent self-diffusion coefficients in binary liquid mixtures: the missing link for Darken-based models, Ind. Eng. Chem. Res. 57 (43) (2018) 14784–14794.

[12] B.E. Poling, J.M. Prausnitz, J.P. O'Connel, The Properties of Gases and Liquids, fifth ed., McGraw-Hill, Singapore, 2001.

[13] X. Liu, S.K. Schnell, J.-M. Simon, P. Krüger, D. Bedeaux, S. Kjelstrup, A. Bardow, T.J.H. Vlugt, Diffusion coefficients from molecular dynamics simulations in binary and ternary mixtures, Int. J. Thermophys. 34 (7) (2013) 1169–1196.

[14] S.H. Jamali, L. Wolff, T.M. Becker, M. de Groen, M. Ramdin, R. Hartkamp, A. Bardow, T.J.H. Vlugt, O.A. Moultos, OCTP: a tool for on-the-fly calculation of transport properties of fluids with the order-n algorithm in LAMMPS, J. Chem. Inf. Model. 59 (4) (2019) 1290–1294.

[15] S.H. Jamali, A. Bardow, T.J.H. Vlugt, O.A. Moultos, Generalized form for finite-size corrections in mutual diffusion coefficients of multicomponent mixtures obtained from equilibrium molecular dynamics simulation, J. Chem. Theory Comput. 16 (6) (2020) 3799–3806.

[16] N. Dawass, P. Krüger, S.K. Schnell, J.-M. Simon, T. Vlugt, Kirkwood-buff integrals from molecular simulation, Fluid Phase Equilib. 486 (2019) 21–36.

[17] N. Dawass, P. Krüger, S.K. Schnell, O.A. Moultos, I.G. Economou, T.J.H. Vlugt, J.-M. Simon, Kirkwood-Buff integrals using molecular simulation: estimation of surface effects, Nanomaterials 10 (4) (2020) 771.

[18] D.M. Himmelblau, Diffusion of dissolved gases in liquids, Chem. Rev. 64 (5) (1964) 527–550.

[19] C.R. Wilke, P. Chang, Correlation of diffusion coefficients in dilute solutions, AIChE J. 1 (2) (1955) 264–270.

[20] A. Boushehri, J. Bzowski, J. Kestin, E.A. Mason, Equilibrium and transport properties of eleven polyatomic gases at low density, J. Phys. Chem. Ref. Data 16 (3) (1987) 445–466.

[21] R.B. Bird, W.E. Stewart, E.N. Lightfoot, Transport Phenomena, second ed., John Wiley & Sons, New York, 2007.

[22] R.S. Brokaw, Predicting transport properties of dilute gases, Ind. Eng. Chem. Proc. Des. Dev. 8 (1969) 240–2530.

[23] M.P. Allen, D.J. Tildesley, Computer Simulation of Liquids, second ed., Oxford University Press, Croydon, 2017.

[24] D. Frenkel, B. Smit, Understanding Molecular Simulation: from Algorithms to Applications, second ed., Elsevier, San Diego, California, 2001.

[25] S. Plimpton, Fast parallel algorithms for short-range molecular dynamics, J. Comput. Phys. 117 (1) (1995) 1–19.

[26] D. Van Der Spoel, E. Lindahl, B. Hess, G. Groenhof, A.E. Mark, H.J.C. Berendsen, GROMACS: fast, flexible, and free, J. Comput. Chem. 26 (16) (2005) 1701–1718.

[27] J.L.F. Abascal, C. Vega, A general purpose model for the condensed phases of water: TIP4P/2005, J. Chem. Phys. 123 (23) (2005) 234505.

[28] M.G. Martin, J.I. Siepmann, Transferable potentials for phase equilibria. 1. United-atom description of n-alkanes, J. Phys. Chem. B 102 (97) (1998) 2569–2577.

[29] H. Jiang, O.A. Moultos, I.G. Economou, A.Z. Panagiotopoulos, Gaussian-charge polarizable and nonpolarizable models for CO₂, J. Phys. Chem. B 120 (5) (2016) 984–994.

[30] R.S. Chatwell, G. Guevara-Carrion, Y. Gaponenko, V. Shevtsova, J. Vrabec, Diffusion of the carbon dioxide–ethanol mixture in the extended critical region, Phys. Chem. Chem. Phys. 23 (2021) 3106–3115.

[31] S. Kozlova, A. Mialdun, I. Ryzhkov, T. Janzen, J. Vrabec, V. Shevtsova, Do ternary liquid mixtures exhibit negative main Fick diffusion coefficients? Phys. Chem. Chem. Phys. 21 (2019) 2140–2152.

[32] V.K. Michalis, O.A. Moultos, I.N. Tsimpanogiannis, I.G. Economou, Molecular dynamics simulations of the diffusion coefficients of light n-alkanes in water over a wide range of temperature and pressure, Fluid Phase Equilib. 407 (2016) 236–242.

[33] S. Päez, G. Guevara-Carrion, H. Hasse, J. Vrabec, Mutual diffusion in the ternary mixture of water + methanol + ethanol and its binary subsystems, Phys. Chem. Chem. Phys. 15 (2013) 3985–4001.

[34] X. Liu, A. Bardow, T.J.H. Vlugt, Multicomponent Maxwell-Stefan diffusivities at infinite dilution, Ind. Eng. Chem. Res. 50 (8) (2011) 4776–4782.

[35] O.A. Moultos, I.N. Tsimpanogiannis, A.Z. Panagiotopoulos, I.G. Economou, Self-Diffusion coefficients of the binary (H₂O + CO₂) mixture at high temperatures and pressures, J. Chem. Thermodyn. 93 (2016) 424–429.

[36] O.A. Moultos, G.A. Orozco, I.N. Tsimpanogiannis, A.Z. Panagiotopoulos, I.G. Economou, Atomistic molecular dynamics simulations of H₂O diffusivity in liquid and supercritical CO₂, Mol. Phys. 113 (17–18) (2015) 2805–2814.

[37] S. Berkowicz, F. Perakis, Exploring the validity of the stokes–einstein relation in supercooled water using nanomolecular probes, Phys. Chem. Chem. Phys. 23 (2021) 25490–25499.

[38] I.N. Tsimpanogiannis, O.A. Moultos, L.F. Franco, M.B.d.M. Spera, M. Erdős, I.G. Economou, Self-diffusion coefficient of bulk and confined water: a critical review of classical molecular simulation studies, Mol. Simul. 45 (4–5) (2019) 425–453.

[39] I.N. Tsimpanogiannis, S.H. Jamali, I.G. Economou, T.J.H. Vlugt, O.A. Moultos, On the validity of the stokes–einstein relation for various water force fields, Mol. Phys. 118 (9–10) (2020) e1702729.

[40] Z. Shi, P.G. Debenedetti, F.H. Stillinger, Relaxation processes in liquids: variations on a theme by stokes and einstein, J. Chem. Phys. 138 (12) (2013) 12A526.

[41] C. Corsaro, E. Fazio, D. Mallamace, The stokes-einstein relation in water/methanol solutions, J. Chem. Phys. 150 (23) (2019) 234506.

[42] D. Bonn, W.K. Kegel, Stokes-Einstein relations and the fluctuation-dissipation theorem in a supercooled colloidal fluid, J. Chem. Phys. 118 (4) (2003) 2005–2009.

[43] A. Einstein, Investigations on the Theory of Brownian Motion, first ed., Dover, New York, 1956.

[44] G. Tarjus, D. Kivelson, Breakdown of the stokes–einstein relation in supercooled liquids, J. Chem. Phys. 103 (8) (1995) 3071–3073.

[45] P. Kumar, S.V. Buldyrev, S.R. Becker, P.H. Poole, F.W. Starr, H.E. Stanley, Relation between the Widom line and the breakdown of the stokes-einstein relation in supercooled water, Proc. Natl. Acad. Sci. 104 (23) (2007) 9575–9579.

[46] S.G. Schultz, A.K. Solomon, Determination of the effective hydrodynamic radii of small molecules by viscometry, J. Gen. Physiol. 44 (6) (1961) 1189–1199.

[47] G. Ren, Y. Wang, Conservation of the stokes–einstein relation in supercooled water, Phys. Chem. Chem. Phys. 23 (2021) 24541–24544.

[48] S. Kraft, F. Vogel, Estimation of binary diffusion coefficients in supercritical water: mini review, Ind. Eng. Chem. Res. 56 (16) (2017) 4847–4855.

[49] E.G. Scheibel, Correspondence. liquid diffusivities. viscosity of gases, Ind. Eng. Chem. 46 (9) (1954) 2007–2008.

[50] K.A. Reddy, L.K. Doraiswamy, Estimating liquid diffusivity, Ind. Eng. Chem. Fundam. 6 (1) (1967) 77–79.

[51] M.A. Lusis, C.A. Ratcliff, Diffusion in binary liquid mixtures at infinite dilution, Can. J. Chem. Eng. 46 (5) (1968) 385–387.

[52] E.W. Lemmon, I.H. Bell, M.L. Huber, M.O. McLinden, NIST Standard Reference Database 23: Reference Fluid Thermodynamic and Transport Properties-REFPROP, Version 10.0, National Institute of Standards and Technology, 2018.

[53] A.L. Magalhães, P.F. Lito, F.A. Da Silva, C.M. Silva, Simple and accurate correlations for diffusion coefficients of solutes in liquids and supercritical fluids over wide ranges of temperature and density, J. Supercrit. Fluids 76 (2013) 94–114.

[54] K.R. Harris, Communications: the fractional stokes–einstein equation: application to water, J. Chem. Phys. 132 (23) (2010) 231103.

[55] T. Kawasaki, K. Kim, Identifying time scales for violation/preservation of stokes-einstein relation in supercooled water, Sci. Adv. 3 (8) (2017) e1700399.

[56] H. Zhao, H. Zhao, Testing the stokes-einstein relation with the hard-sphere fluid model, Phys. Rev. E 103 (2021) L030103.

[57] I.-C. Yeh, G. Hummer, System-size dependence of diffusion coefficients and viscosities from molecular dynamics simulations with periodic boundary conditions, J. Phys. Chem. B 108 (40) (2004) 15873–15879.

[58] A.T. Celebi, S.H. Jamali, A. Bardow, T.J.H. Vlugt, O.A. Moultos, Finite-size effects of diffusion coefficients computed from molecular dynamics: a review of what we have learned so far, Mol. Simul. 47 (10–11) (2021) 831–845.

[59] B. Dünweg, K. Kremer, Molecular dynamics simulation of a polymer chain in solution, J. Chem. Phys. 99 (9) (1993) 6983–6997.

[60] S.H. Jamali, L. Wolff, T.M. Becker, A. Bardow, T.J.H. Vlugt, O.A. Moultos, Finite-size effects of binary mutual diffusion coefficients from molecular dynamics, J. Chem. Theory Comput. 14 (5) (2018) 2667–2677.

[61] M. Erdős, M. Frangou, T.J. Vlugt, O.A. Moultos, Diffusivity of α-, β-, γ-cyclodextrin and the inclusion complex of β-cyclodextrin: ibuprofen in aqueous solutions; a molecular dynamics simulation study, Fluid Phase Equilib. 528 (2021) 112842.

[62] S.H. Jamali, R. Hartkamp, C. Bardas, J. Söhl, T.J.H. Vlugt, O.A. Moultos, Shear viscosity computed from the finite-size effects of self-diffusivity in equilibrium molecular dynamics, J. Chem. Theory Comput. 14 (11) (2018) 5959–5968.

[63] O.A. Moultos, Y. Zhang, I.N. Tsimpanogiannis, I.G. Economou, E.J. Maginn, System-size corrections for self-diffusion coefficients calculated from molecular

dynamics simulations: the case of CO_2, n-alkanes, and poly (ethylene glycol) dimethyl ethers, J. Chem. Phys. 145 (7) (2016) 074109.

[64] A. Dehaoui, B. Issenmann, F. Caupin, Viscosity of deeply supercooled water and its coupling to molecular diffusion, Proc. Natl. Acad. Sci. 112 (39) (2015) 12020–12025.

[65] V. Buch, Path integral simulations of mixed para-D_2 and ortho-D_2 clusters: the orientational effects, J. Chem. Phys. 100 (10) (1994) 7610–7629.

[66] M. Bohn, R. Lustig, J. Fischer, Description of polyatomic real substances by two-center Lennard-Jones model fluids, Fluid Phase Equilib. 25 (1986) 251–262.

[67] J. Winkelmann, Landolt-Börnstein: Numerical Data and Functional Relationships in Science and Technology, Group IV: Physical Chemistry Volume 15, Subvolume A: Gases in Gases, Liquids and their Mixtures, Springer-Verlag, Berlin/Heidelberg/New York, 2007.

[68] K.H. Gertz, H.H. Loeschcke, Bestimmung der Diffusions-Koeffizienten von H_2, O_2, N_2, und He in Wasser und Blutserum bei konstant gehaltener Konvektion, Z. Naturforsch. B 9 (1) (1954) 1–9.

[69] M.H. Baird, J.F. Davidson, Annular jets—II: gas absorption, Chem. Eng. Sci. 17 (6) (1962) 473–480.

[70] D.L. Wise, G. Houghton, The diffusion coefficients of ten slightly soluble gases in water at 10–60 °C, Chem. Eng. Sci. 21 (11) (1966) 999–1010.

[71] A. Akgerman, J.L. Gainer, Predicting gas-liquid diffusivities, J. Chem. Eng. Data 17 (3) (1972) 372–377.

[72] W.J. de Blok, J.M.H. Fortuin, Method for determining diffusion coefficients of slightly soluble gases in liquids, Chem. Eng. Sci. 36 (10) (1981) 1687–1694.

[73] P. Verhallen, L. Oomen, A. Elsen, J. Kruger, J. Fortuin, The diffusion coefficients of helium, hydrogen, oxygen and nitrogen in water determined from the permeability of a stagnant liquid layer in the quasi-steady state, Chem. Eng. Sci. 39 (11) (1984) 1535–1541.

[74] R.T. Ferrell, D.M. Himmelblau, Diffusion coefficients of nitrogen and oxygen in water, J. Chem. Eng. Data 12 (1) (1967) 111–115.

[75] P. Han, D.M. Bartels, Temperature dependence of oxygen diffusion in h_2o and d_2o, J. Phys. Chem. 100 (13) (1996) 5597–5602.

[76] W. Wagner, A. Pruss, International equations for the saturation properties of ordinary water substance. revised according to the international temperature scale of 1990. Addendum to J. Phys. Chem. Ref. Data 16 (1987) 893, J. Phys. Chem. Ref. Data 22 (3) (1993) 783–787.

[77] C. Vega, J.L.F. Abascal, Simulating water with rigid non-polarizable models: ageneral perspective, Phys. Chem. Chem. Phys. 13 (44) (2011) 19663–19688.

[78] G. Guevara-Carrion, R. Fingerhut, J. Vrabec, Diffusion in multicomponent aqueous alcoholic mixtures, Sci. Rep. 11 (2021) 12319.

[79] G. Guevara-Carrion, Y. Gaponenko, T. Janzen, J. Vrabec, V. Shevtsova, Diffusion in multicomponent liquids: from microscopic to macroscopic scales, J. Phys. Chem. B 120 (47) (2016) 12193–12210.

[80] H. S. Salehi, A.T. Celebi, T.J.H. Vlugt, O.A. Moultos, Thermodynamic, transport, and structural properties of hydrophobic deep eutectic solvents composed of tetraalkylammonium chloride and decanoic acid, J. Chem. Phys. 154 (14) (2021) 144502.

[81] N. Dawass, J. Langeveld, M. Ramdin, E. Pérez-Gallent, A.A. Villanueva, E.J. M. Giling, J. Langerak, L.J.P. van den Broeke, T.J.H. Vlugt, O.A. Moultos, Solubilities and transport properties of CO_2, oxalic acid, and formic acid in mixed solvents composed of deep eutectic solvents, methanol, and propylene carbonate, J. Phys. Chem. B 126 (19) (2022) 3572–3584.

[82] A.T. Celebi, T.J.H. Vlugt, O.A. Moultos, Structural, thermodynamic, and transport properties of aqueous reline and ethaline solutions from molecular dynamics simulations, J. Phys. Chem. B 123 (51) (2019) 11014–11025.

[83] F. Kapteijn, J. Moulijn, R. Krishna, The generalized Maxwell–Stefan model for diffusion in zeolites:: sorbate molecules with different saturation loadings, Chem. Eng. Sci. 55 (15) (2000) 2923–2930.

[84] D. Dubbeldam, R.Q. Snurr, Recent developments in the molecular modeling of diffusion in nanoporous materials, Mol. Simul. 33 (4–5) (2007) 305–325.

[85] E. Beerdsen, B. Smit, Understanding diffusion in nanoporous materials, in: R. Xu, Z. Gao, J. Chen, W. Yan (Eds.), From Zeolites to Porous MOF Materials - The 40th Anniversary of International Zeolite Conference, Studies in Surface Science and Catalysis, vol. 170, Elsevier, 2007, pp. 1646–1651.

[86] R. Krishna, J.M. van Baten, E. García-Pérez, S. Calero, Incorporating the loading dependence of the Maxwell-Stefan diffusivity in the modeling of CH_4 and CO_2 permeation across zeolite membranes, Ind. Eng. Chem. Res. 46 (10) (2007) 2974–2986.